Monolayer Freeze-fracture Autoradiography: Quantitative Analysis of the Transmembrane Distribution of Radioiodinated Concanavalin A

KNUTE A. FISHER
Department of Biochemistry and Biophysics, and Cardiovascular Research Institute, University of California, San Francisco, California 94143

ABSTRACT The technique of monolayer freeze-fracture autoradiography (MONOFARG) has been developed and the principles, quantitation, and application of the method are described. Cell monolayers attached to polylysine-treated glass were freeze-fractured, shadowed, and coated with dry, Parlodion-supported Ilford L4 photographic emulsion at room temperature. Quantitative aspects of MONOFARG were examined using radioiodinated test systems. Background was routinely $<2.5 \times 10^{-4}$ grains/μm^2/day, the highest overall efficiency was between 25% and 45%, and grain density and efficiency were dependent on radiation dose for iodine-125 and D-19 development. Corrected grain densities were linearly proportional to iodine-125 concentration. The method was applied to an examination of the transmembrane distribution of radioiodinated and fluoresceinated concanavalin A (^{125}I-FITC-Con-A). Human erythrocytes were labeled, column-purified, freeze-dried or freeze-fractured, autoradiographed, and examined by electron microscopy. The number of silver grains per square micrometer of unsplit single membrane was essentially identical to that of split extracellular membrane "halves." These data demonstrate that ^{125}I-FITC-Con-A partitions exclusively with the extracellular "half" of the membrane upon freeze-fracturing and can be used as a quantitative marker for the fraction of extracellular split membrane "halves." This method should be able to provide new information about certain transmembrane properties of biological membrane molecules and probes, as well as about the process of freeze-fracture per se.

MONOFARG is the combination of monolayer freeze-fracture (14, 15) and electron microscope autoradiography (16–18). In monolayer freeze-fracture, cell plasma membranes attached to planar cationic surfaces fracture preferentially to produce large areas of split membrane E-faces (4). In principle, the production of such surfaces, being based on a physical fractionation approach, offers a unique opportunity to study the transbilayer distribution of diffusible and extractable molecules (17, 18). In practice, the fractured single "half" membranes are especially well-suited to study by electron microscopic autoradiography.

The methodological advantages of MONOFARG are several (17, 18). The areas of "half" membranes are extraordinarily large (cm^2 dimensions) by transmission electron microscopy (TEM) standards. The source of radioisotope can be unequivocally identified, because TEM confirms that shadowed radiolabeled split membranes do not lie on top of other sources of radioactivity. The surfaces are planar, ideal for autoradiography (ARG), allowing close and reproducible contact between source and detector. Finally, because split membranes attached to PL-glass are physically supported, they can be freeze-dried (deep-etched) and processed after shadowing by conventional ARG techniques such as room temperature coating and exposure at 5°C (16–18). These features clearly distinguish MONOFARG from earlier attempts to combine conventional freeze-fracturing with TEM ARG at low temperature (13, 23, 24, 34, 46, 47). The technical advantages of the MONOFARG approach have also been recognized by several other investigators (30, 48) who have additionally established its qualitative feasibility.

As originally conceived (16), MONOFARG was intended to be a quantitative tool used to determine the amount of radioisotopic probe in split and intact membranes. Nevertheless, a direct examination of the quantitative feasibility of the method is lacking for both transmembrane and in-plane analyses,

THE JOURNAL OF CELL BIOLOGY · VOLUME 93 APRIL 1982 155-163

especially in the areas of ARG efficiency and dose dependence. Moreover, the effect on quantitative analyses of a platinum-carbon replica interposed between radioisotope and detector is a special concern. The present report provides quantitative data for MONOFARG using radioiodinated (^{125}I) test systems.

Recently, a method for measuring quantities of split membrane "halves" by absorbance and fluorescence spectroscopy was described (19, 22). In that method, called double labeled membrane splitting, hemoglobin absorbance was used as a marker for the cytoplasmic side of the membrane, and fluoresceinated concanavalin A (FITC-Con-A) fluorescence as a marker for the extracellular side. While double labeled membrane splitting has an advantage of being more rapid than techniques based on quantitative electron microscopy, it is based on the assumption that FITC-Con-A partitions exclusively with the extracellular surface (ES) (4), upon freeze-fracturing. Here MONOFARG has been used to examine that assumption. Results clearly show that, for human erythrocytes labeled with radioiodinated FITC-Con-A, the radioisotope remains quantitatively associated with the extracellular "half" of the membrane after freeze-fracturing.

MATERIALS AND METHODS

A synopsis of the MONOFARG technique is given in Fig. 1. Details of the preparation of FITC-Con-A-labeled human erythrocytes (RBC's), cell monolayer formation on polylysine treated 11 × 22-mm cover glasses (PL-glass), and quantitative fracturing properties have been described (21, 22). The following section describes details of the MONOFARG technique, preparation of the ^{125}I-FITC-Con-A label, PL-glass test system, and RBC labeling and ghost (RBCG) formation for transmembrane analysis.

MONOFARG Technique

TUBE PREPARATION: Parlodion-supported monolayers of nuclear emulsion were prepared following the principles of the flat substrate method (5, 39). Parlodion films were formed at an air-water interface (13, 24). Floating films that were homogeneously transparent or showed silver-gray interference colors in reflected light were selected for transfer. Films were transferred to open-ended glass tubes (3.0-cm ID × 3.5-cm OD × 5.0-cm long) by gently pressing one end of the tube against the floating film and using a submerged 4.2-cm (ID) nichrome wire loop to draw the edges of the film up along the outside surface of the tube. Parlodion-coated tubes were tipped slightly, withdrawn from the water surface, and set horizontally to allow the films to air dry vertically for several hours. The inside surface of the Parlodion film was coated ("subbed") with 0.25% (wt/vol) gelatin dissolved in boiling glass-distilled water and cooled to 20 to 30°C. 1 ml was carefully pipetted into the tube, swirled over the entire surface of the Parlodion film, and the excess poured off. Tubes were again positioned horizontally so that the gelatin would drain vertically. When visibly dry, tubes were transferred to a photographic darkroom for coating with emulsion. The thickness of the dry, gelatin-subbed Parlodion film could be evaluated by transferring the film to a glass disk. Silver to gold interference colors indicate a combined thickness of 50 to 100 nm.

EMULSION PREPARATION: Gelatin-subbed Parlodion films were equilibrated in a temperature and humidity (~85% relative humidity) chamber by placing them on pegs inside the chamber hood over a 41°C waterbath (Fig. 2). Darkroom safelight was provided by a 15-W bulb, variac regulated to 57 V maximum, through a Kodak Wratten OC filter at a distance of at least 84 cm (maximum light intensity was 4 μW cm^{-2}). Ilford L4 autoradiographic emulsion (Ilford Ltd., Essex, England) was weighed into a 70-mm crystallizing dish, diluted with four parts glass-distilled water (e.g., 6 g of emulsion plus 24 ml of water), placed and gently stirred in a waterbath at 50°C for 3 min. The dish of emulsion was transferred to the coating chamber water bath (41°C) and stirred for 5 min. Tubes were removed from their posts in the chamber, tilted at a slight angle, and the Parlodion-film-coated end dipped into the emulsion. The tubes were gently swirled for a few seconds, removed, and returned to their posts to drain vertically. After 30 to 60 min, tubes were transferred to a light-tight storage box at ambient temperature and humidity, and applied to samples within 24 h.

SHADOWED SAMPLE PREPARATION: In room light, strips (1.5 to 2-mm wide × 11-mm long) were cut from platinum-carbon (Pt-C) shadowed samples on 11 × 22-mm PL-glass and attached at one end to a narrow strip of double stick tape on a 25-mm Diam round cover glass, usually four to seven samples per disk. Radioactive samples and nonradioactive controls were arranged side by side on a single disk, which was then transferred to a cylindrical pedestal (2.9-cm OD × 5.3-cm high). Disks were oriented such that the long axes of the sample strips were parallel to the direction of emulsion draining, so that adjacent areas of

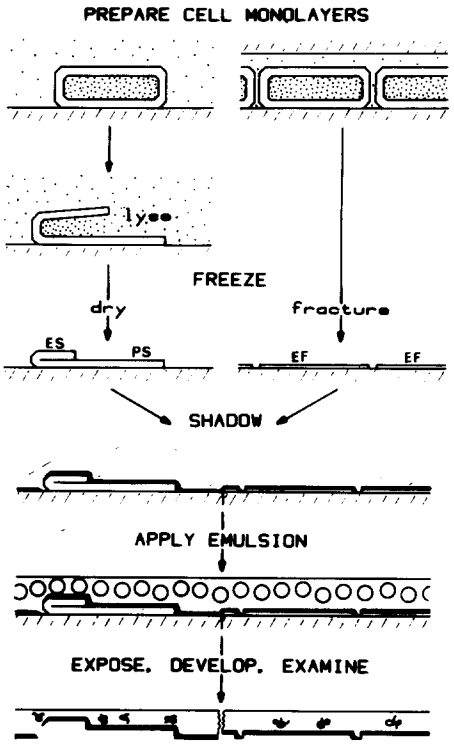

FIGURE 1 MONOFARG, a synopsis of the technique. Cells labeled with radioisotope are attached to PL-glass and either lysed and freeze-dried (*left*), or freeze-fractured (*right*). From this point intact (*left*) and split (*right*) membrane preparations are paired and processed together so that they receive the same quality and quantity of Pt-C replica, ARG emulsion, and photographic processing. The transmembrane distribution of a radioisotope is determined by comparing the silver grain densities overlying intact membranes of single or double thickness (*lower left*) with those over split membranes (*lower right*). *ES:* extracellular surface; *PS:* cytoplasmic surface; *EF:* extracellular split membrane "half."

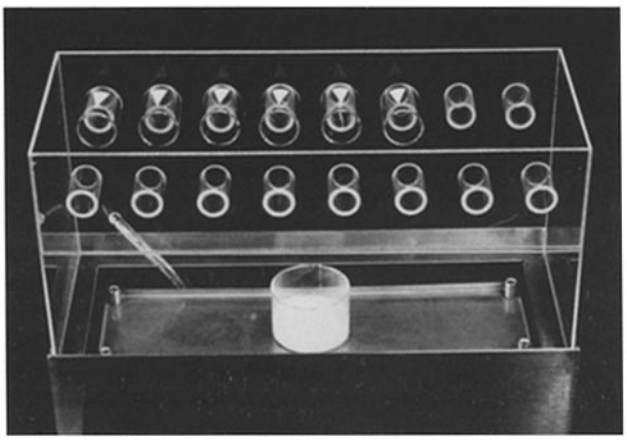

FIGURE 2 Emulsion coating chamber. Plexiglass hood (20 cm high × 18 cm wide × 44 cm long) contains 16 pegs for hanging glass tubes and sits atop a water bath. Parlodion-filmed tubes (six shown on rear pegs) are stored in the chamber before and after coating with diluted emulsion shown in the crystallizing dish. The uppermost outer wall of each tube was marked with a white triangle to indicate orientation during drying and application.

control and experimental samples would be covered with the same thickness of emulsion.

FILM APPLICATION AND EXPOSURE: Under safelight the emulsion tube was removed from storage. Both the gelatin subbing and the samples were breath-moistened, and the tubes were lowered over the samples on the pedestal, with gelatin subbing nearest the replicas. While in contact with the replica the Parlodion-emulsion was freed from the perimeter of the tube. A cross-sectional diagram, drawn to scale, of a split membrane-replica-emulsion sandwich is shown in Fig. 3. The emulsion-coated disks were taped to glass microscope slides and placed in a light-tight box containing anhydrous dessicant (W. A. Hammond Drierite Co., Xenia, OH). Boxes were taped and transferred to a refrigerator for exposure at 5°C.

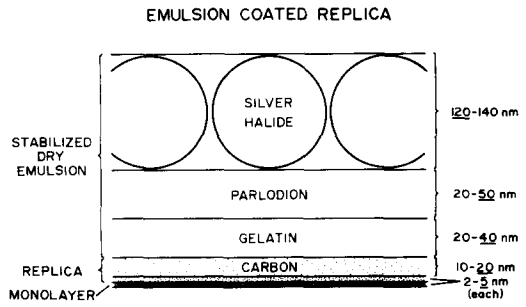

FIGURE 3 Idealized scale diagram of MONOFARG stripping film applied to a replicated sample. Illustrated thicknesses are underlined.

PHOTOGRAPHIC PROCESSING: After exposure, slides were placed in a glass staining rack, and multiple samples were processed simultaneously in 200 ml of photographic solutions, equilibrated to 20°C in a water-bath. Samples were developed in undiluted D-19 (Eastman Kodak Co., Rochester, NY) for 2 or 4 min, as noted, with gentle agitation every 10 s, rinsed in glass-distilled water for 30 s and in 3% (vol/vol) acetic acid for 15 s, fixed with 20% (wt/vol) sodium thiosulfate plus 2.5% (wt/vol) potassium metabisulfite for 5 min, washed in tempered running water for 10 min, and finally in glass-distilled water for 1 min.

ELECTRON MICROSCOPY: Air-dried emulsion-coated replicas were cut into 2 × 2-mm squares, floated off the glass onto diluted HF (HF:water, 1:1), quickly transferred by loop through three floats on glass-distilled water, and picked up on uncoated, flamed 200-mesh grids. No further sample cleaning was necessary. Samples were examined in a Siemens 101 electron microscope and photographed at random. In the transmembrane distribution studies, individual RBCG's were randomly selected, then positioned to fill the viewing screen; split membrane samples were selected only to avoid partially fractured areas. Micrographs, 154 to 170 μm^2/micrograph and 5 to 24 micrographs per sample, were taken at magnifications ranging from 5,500 to 5,700 times. A micrograph of a cross-ruled replica grating calibration standard was taken with every set of 36 exposures.

ANALYSIS: Micrographs were routinely prepared at a final print magnification of 16,000 times. All developed silver grains were tabulated. Intertwined grains were subjectively scored as equal to one to a maximum of three grains; such aggregates represented less than a few percent of the total number of grains counted. Areas were measured with a calibrated compensating polar planimeter (Model 620015, Keuffel and Esser Co., Morristown, NJ). Because all potential source compartments were large compared to the estimated resolution of the technique (20), the simple grain density method of analysis (39, 40, 45) was used. In labeled unsplit or split membrane preparations, grains that lay directly over or within 0.5 μm of the edge of the membrane were assigned to that membrane. Since the resolution of MONOFARG has not yet been unequivocally determined (20), an estimated half distance (HD) value of 150 nm was assumed. Silver grain densities were derived from counts of silver grains overlying PL-glass. Areas of 30-nm wide bands parallel to, and up to 1.2 μm from, the perimeters of RBCG's were measured by planimetry. Grain densities normalized to unity at a ± 1 HD bin centered at the edge of the RBCG membrane were plotted as a function of the distance divided by the HD.

^{125}I-FITC-Con-A Preparation

Radioiodinated derivatives of FITC-Con-A were prepared following the Bolton Hunter procedure (3). FITC-Con-A (Vector Laboratories Inc., Burlingame, CA), 100 μg in 10 μl of 0.1 M borate buffer, pH 8.5, was added to 1 mCi of nitrogen-dried, radioiodinated *p*-hydroxyphenylpropionic acid *N*-hydroxysuccinimide ester in a combi-vial (Bolton Hunter Reagent, sp act 2,000 Ci/mmol; New England Nuclear, Boston, MA) and incubated on ice for 60 min with occasional swirling, then stored at 5°C in the dark for 24 h. The radioiodinated sample was applied to a Sephadex G-25 column equilibrated with 50 mM phosphate-buffered saline, PBS (15), containing 0.25% gelatin and 0.02% sodium azide followed by two 10-μl washes of the vial. Void volume fluorescence was monitored with a UV lamp, and fluorescent fractions were pooled to a final volume of ~500 μl. Specific activity of the radioiodinated FITC-Con-A was ~0.4 mCi/mg.

PL-Glass Test System

Several-month-old ^{125}I-FITC-Con-A, no longer suitable for RBC labeling due to aggregation and decreased specific activity, was used to prepare a test system. Dilutions of ^{125}I-FITC-Con-A were applied to 11 × 22-mm PL-glasses for 90 s, 20°C, rinsed for 30 s, nitrogen dried, shadowed or not, and cut into strips.

Some ^{125}I-FITC-Con-A treated glasses were shadowed with Pt-C at an angle of 20° in a Varian vacuum evaporator. Shadowed and unshadowed glasses were cut into strips for liquid scintillation counting (LSC) and ARG. Those for LSC were placed in an enlarger and prints were made at an enlargement of either 10.5 or 15.9 times. Areas of the glass were measured by planimetry of the prints. Glasses were floated, replica side down, on droplets (usually 40 μl) of diluted HF (HF:water, 1:1) on the sides of plastic scintillation vials for 30 s before adding 10 ml Aquasol-2 (New England Nuclear).

To monitor recovery of activity from the PL-glass, detergent- as well as HF-treated glasses were examined. ^{125}I-FITC-Con-A (20 μl) was added to 10 ml of Aquasol-2 or to 2.5 ml of SDS-borate buffer (1% wt/vol SDS in 10 mM sodium tetraborate, pH 9.5), dried at 75°C under flowing air for 60 min, cooled, and resuspended in 10-ml cocktail with sonication (22). Similarly, 20-μl portions were applied to PL-glasses and allowed to air-dry for 30 to 40 min at RT before being dropped into 2.5 ml of SDS-borate, dried, and resuspended in Aquasol-2 as above. FITC-fluorescence was measured as previously described (22).

Radioactivity was measured with an LS-7000 scintillation counter (Beckman Instruments, Inc., Fullerton, CA) optimized for ^{125}I (counter efficiency = 77%). Background counts from nonradioactive controls were subtracted from matching ^{125}I-labeled glasses. The scintillation counter was calibrated with, and quench curves prepared using, ^{125}I standards (New England Nuclear).

For ARG, glass strips, shadowed or not, were coated with Parlodion-supported emulsion, processed, and examined as described. No correction was made for the occurrence of multiple emissions during each nuclear disintegration (25, 44). Decays per minute (dpm) were determined as previously described by Fertuck and Salpeter (12) where *dpm = cpm/counter efficiency*. A second evaluation of MONOFARG efficiency was derived from ^{125}I-FITC-Con-A-labeled RBC's.

RBC Labeling and Cell Monolayer Evaluation

A+ human erythrocytes were labeled with ^{125}I-FITC-Con-A (22). Briefly, in a standard preparation, 200 μl of pelleted, washed RBC's were incubated with 30 μg of ^{125}I-FITC-Con-A in a final volume of 2.5 ml of HEPES-buffered saline (HBS), pH 7.4, containing 1 mM Ca^{++} and 1 mM Mg^{++} for 90 min on ice. Cells were diluted to 15 ml, pelleted, and applied to a Bio-Gel A-15m column (Bio-Rad Laboratories, Richmond, CA). RBC fractions were pooled, pelleted, and resuspended to final volumes of either 2 vol cells plus 1 vol HBS for standard freeze-fracture preparations, or to 1 vol cells plus 5 vol HBS for ghost monolayer preparation.

Specific activities of cells in suspension, before monolayer formation, were determined by scintillation counting, and number of cells by both hemacytometry and Hb absorbance measurements (22). Cell surface dpd/μm^2 was calculated using the value of 140 μm^2 surface area per RBC (14) and total number of disintegrations by integrating dpd/μm^2 for times ranging to 63 d.

Cell monolayers attached to PL-glass were prepared and ghosted as previously described (22). In these experiments, photomicrographs of cells or ghosts were taken immediately before spectroscopic measurements. Cell monolayers attached to PL-glass were placed against a second 11 × 22-mm glass. To avoid loss of Hb absorbance or ^{125}I radioactivity after light microscopy, the entire cover glass sandwich was dropped into 2.5 ml of SDS-borate and sonicated. Absorbance was measured at 403 nm, and samples were dried, resuspended in Aquasol-2, and radioactivity was measured. For MONOFARG, either ghosted or intact cell monolayers were prepared, ghosts freeze-dried and RBC's freeze-fractured, and samples paired and simultaneously shadowed (see Fig. 1 and reference 22).

RESULTS

MONOFARG Technique

The glass tubes provided a convenient support for the Parlodion films and a means of orienting the Parlodion and emulsion films during drying and application. Use of the

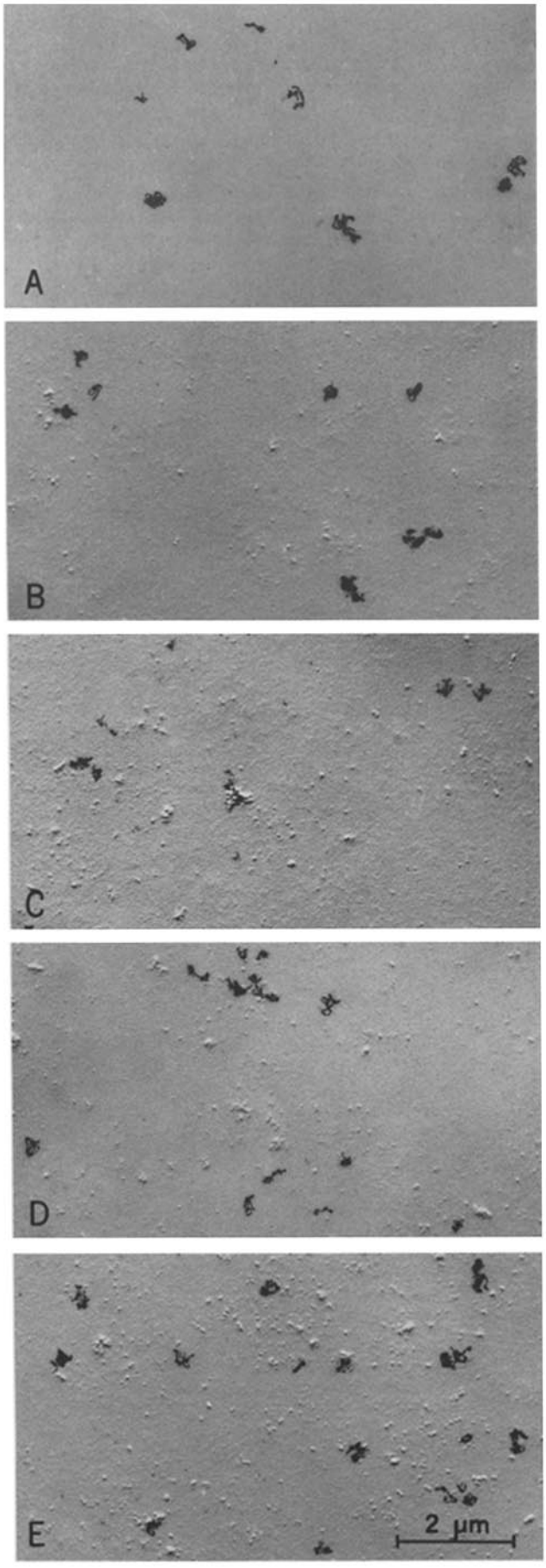

coating chamber significantly improved emulsion monolayer reproducibility and reduced background, presumably by providing a controllably warm, humid, and draft-free environment for draining and slow drying (2). Because the area of the Parlodion film was large, there was a gradient of emulsion thickness from top (thinner) to bottom (thicker) with a desirable monolayer band, crescent-shaped and ~1-cm wide, near the center. Emulsions were examined in the safelight before application, and, of every ten tubes prepared, usually six to seven were selected as identical in appearance and evenly homogeneous. The monolayers used for this study were thinner (pale gold interference colors) than the optimum thickness (deep purple) for sensitivity studies (12, 44). Interference colors on test cover glasses to which Parlodion-emulsion films had been applied were observed under normal room light. Silver halide distributions were monitored by TEM of dry films applied to uncoated grids. Orientation of emulsion relative to sample position was easily achieved in the darkroom with the tube and sample-pedestal combination. Subbing the film with gelatin prevented lateral displacement of the films during processing. A disadvantage of the dry film technique was that, during application, small air bubbles could be trapped between film and substrate. These usually covered <5% of the total surface, however, and could be avoided with practice.

Background

Background data was routinely determined for nonradioactive samples exposed for several time periods. PL-glass surfaces with and without attached cells or "half" membranes, and with and without platinum-carbon replicas, showed identical background levels. The background values for the Parlodion-supported emulsion and photographic conditions described in this report lay between 0.7×10^{-4} and 2.5×10^{-4} grains/μm^2 per d (equivalent to a maximum of 1 grain/100 μm^2 per 40 d).

Efficiency and Dose Dependence

Examples of autoradiographs used for ARG efficiency evaluation are shown in Fig. 4. Aggregates of ^{125}I-FITC-Con-A attached to the PL-glass surfaces are clearly visible. The height of most aggregates ranged between 15 and 30 nm, estimated from shadow angle and length. The frequency of aggregate occurrence was proportional to the concentration of ^{125}I-FITC-Con-A applied, for applications of 3, 6, and 12 μg in 25- or 50μl volumes. Note that silver grains are nonrandomly distributed, often lying near large aggregates. A direct comparison of unshadowed (Fig. 4*A*) with shadowed (Fig. 4*B*) samples revealed that the Pt-C shadow had a relatively small effect on silver grain density (also see Fig. 5*B*, *C*).

MONOFARG efficiency data for ^{125}I-FITC-Con-A are given in Table I. In the experiment where PL-glass was treated directly with the ^{125}I-FITC-Con-A, sample activity in dpd/μm^2 PL-glass surface was measured both before and after Pt-C shadowing. Recovery of radioactivity and fluorescence from

FIGURE 4 MONOFARG ^{125}I efficiency test system: ^{125}I-FITC-Con-A applied to PL-glass and autoradiographed. Initial surface activities in dpd/μm^2 were (*A*, *B*) 0.092, (*C*) 0.110, (*D*) 0.187, and (*E*) 0.437. Con A aggregates and silver grain densities are representative of those evaluated. *A*, not shadowed; *B–E*, shadowed with Pt-C; shadow direction bottom to top. All exposed at 5°C for 14 d and developed in undiluted D-19 for 4 min at 20°C. × 9,100.

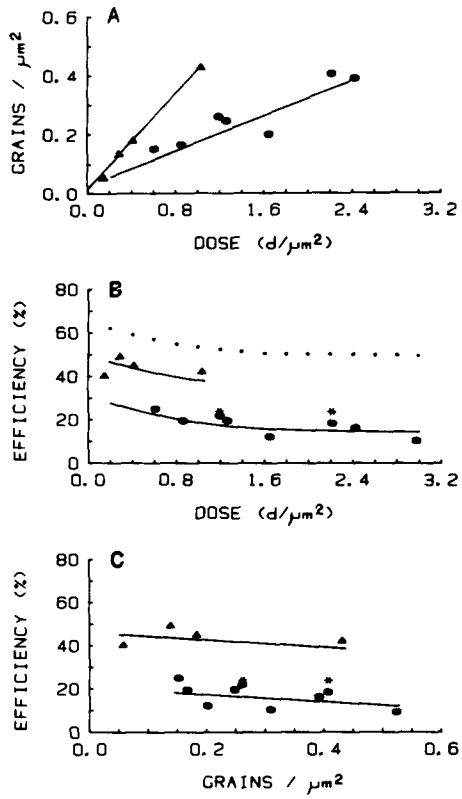

FIGURE 5 MONOFARG data. Scatter diagrams of grain density (*A*) and efficiency (*B*) versus dose expressed as decays (*d*) per μm^2, and as efficiency versus grain density (*C*). Triangles represent ^{125}I-FITC-Con-A-labeled split membrane preparations; circles represent shadowed ^{125}I-FITC-Con-A on PL-glass; asterisks represent unshadowed ^{125}I-FITC-Con-A on PL-glass. Dotted curve in (*B*) derived from Fig. 1 of Fertuck and Salpeter (12). Erythrocyte preparations were exposed for 7, 14, 21, and 63 d, developed in D-19 for 2 min at 20°C; PL-glass preparations were exposed for 7, 14, and 28 d, developed in D-19 for 4 min at 20°C.

labeled Con A adsorbed to PL-glass, after being slowly air-dried, was evaluated. Scrubbing with SDS and sonication recovered 84% of the fluorescence and 80% of the radioactivity applied to the PL-glass; ~20% remained adsorbed to the PL-glass surface. HF treatment, necessary for detaching the Pt-C replica from the glass surfaces, was even less efficient, recovering only 62% from nonreplicated areas and 43% from Pt-C areas. ARG efficiency ranged from 9% to 25% for the PL-glass test system, with highest efficiency corresponding to lowest dose. Even higher efficiencies, ranging from 40% to 48%, were calculated for the RBC system.

Fig. 5 shows three plots of grain density, dose, and efficiency that include much of the data given in Table I. Fig. 5 *A* shows linear relationships between grain density and dose for both the PL-glass (circles) and split RBC (triangles) systems. Fig. 5 *B*, a plot of percent efficiency versus dose, shows that some dose dependence does occur. The data for the two systems

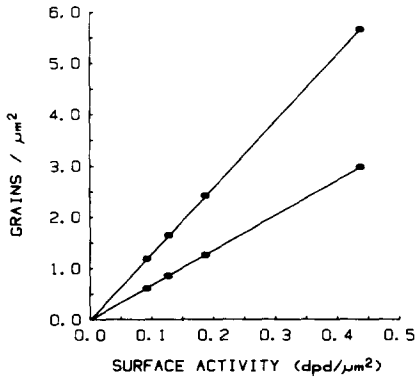

FIGURE 6 Grain density plotted versus initial surface activity of ^{125}I-FITC-Con-A adsorbed to PL-glass. Grain densities corrected for dose dependence for two exposure times: 7 d, lower line, and 14 d, upper line.

TABLE I

MONOFARG Efficiency

^{125}I-FITC-Con A PL-Glass								
Dose				Grain density				
cpm/mm²	dpd/μm²	Exposure	Total decays/μm²	Pictures	Grain	Area	Corrected grains/μm²	Efficiency
		d		*n*	*n*	μm²		%
48.9 ± 10.1	0.092 ± 0.019	7	0.6 ± 0.1	10	246	1,625	0.15 ± 0.04	25 ± 6
(*n* = 12)		14	1.2 ± 0.2	10	438	1,680	0.26 ± 0.06	22 ± 5
		28	2.2 ± 0.5	10	649	1,605	0.41 ± 0.04	18 ± 2
67.9 ± 8.5	0.127 ± 0.016	7	0.9 ± 0.1	5	131	785	0.17 ± 0.05	20 ± 6
(*n* = 4)		14	1.6 ± 0.2	5	161	800	0.20 ± 0.02	12 ± 1
100.0 ± 10.4	0.187 ± 0.019	7	1.3 ± 0.1	5	194	785	0.25 ± 0.03	20 ± 3
(*n* = 4)		14	2.4 ± 0.2	15	962	2,460	0.39 ± 0.07	16 ± 3
220.0 ± 52.5	0.437 ± 0.100	7	3.0 ± 0.7	19	951	3,084	0.31 ± 0.07	10 ± 2
(*n* = 4)		14	5.7 ± 1.3	5	419	800	0.52 ± 0.05	9 ± 1
^{125}I-RBC Splits (E-faces)								
1.146 ± 0.031	0.022 ± 0.001	7	0.15	5	39	653	0.06 ± 0.03	40 ± 19
× 10^{-3} cpm/cell		14	0.29	21	379	2,659	0.14 ± 0.04	48 ± 14
(*n* = 2)		21	0.41	5	124	681	0.18 ± 0.06	44 ± 16
		63	1.03	29	1,333	2,980	0.44 ± 0.09	43 ± 9

PL-GLASS DATA. Corrected dpd/μm^2 and integrated total dose based on: PL-glass area measurement by planimetry of enlarged photographic prints (*n* = number of prints); LSC efficiency = 77%; grain density corrected for background. Some data expressed as mean ± SD. HF recovery from unshadowed PL-glass = 65%. RBC DATA. Number of RBC's determined from absorbance and hemacytometry (*n* = number of experiments). RBC surface area = 140 μm^2.

follow a dose dependence curve given by Fertuck and Salpeter (12) and replotted here (dotted line) for comparison. The curve is derived from their Fig. 1 (12) for ^{125}I-exposed Ilford L4 emulsion developed in Elon-ascorbic acid after gold latensification (42). Although MONOFARG efficiency for the experiments included in this report is clearly less than the optimum (Fig. 5 *B*), the presence or absence (asterisks) of replica appears to play a quantitatively minor role in this decreased efficiency.

The calculated efficiency for the RBC system is much higher than that for the PL-glass test system. Fig. 5 *C* shows the curve used to determine the percent efficiency, given the grain density of a particular sample. Such corrections were applied to data from the PL-glass system for exposures of 7 and 14 d, and corrected grain density was plotted versus surface activity of ^{125}I-FITC-Con-A (Fig. 6) measured by LSC at the start of ARG exposure. Up to 0.5 dpd/μm^2 the corrected grain density

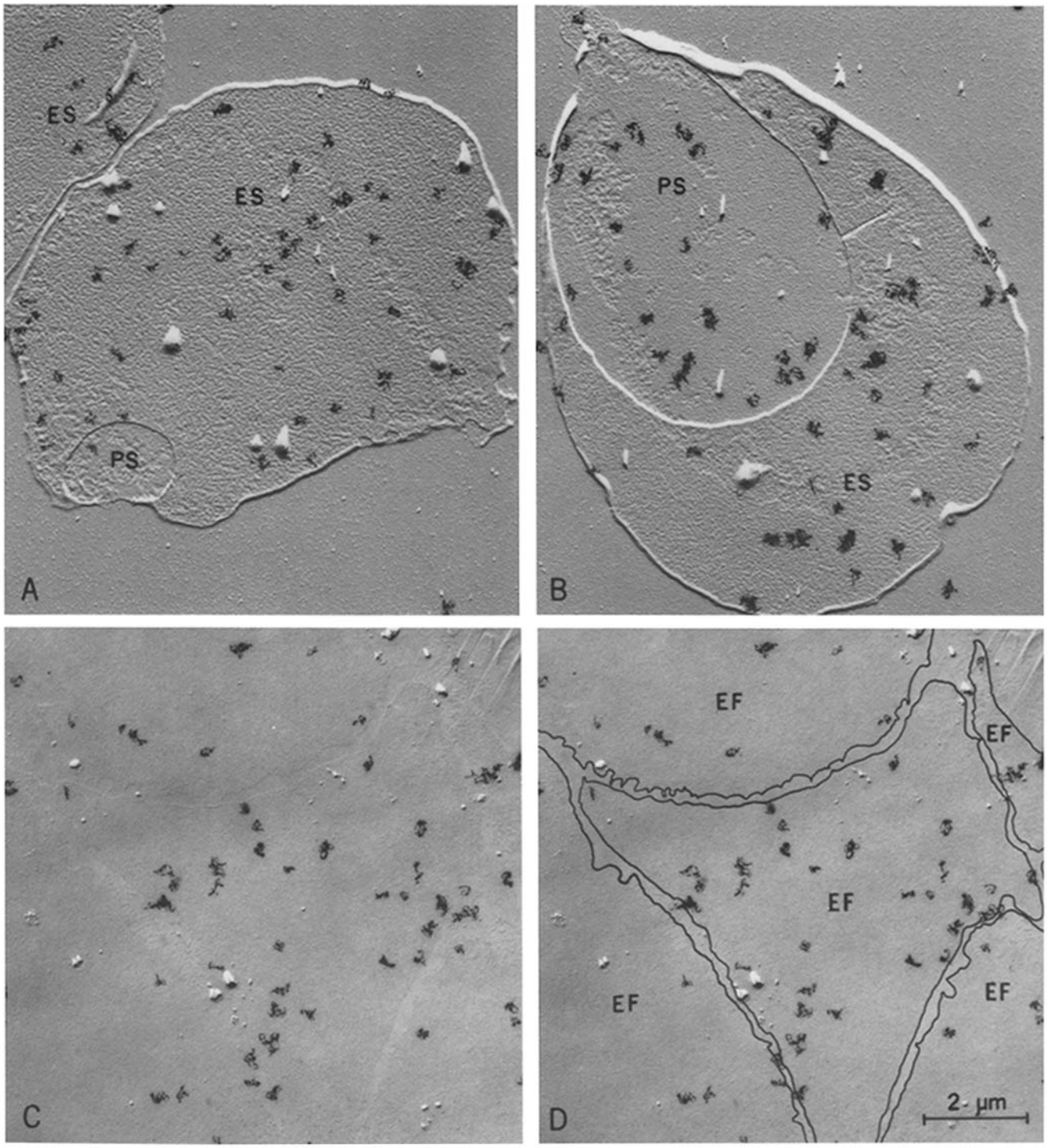

FIGURE 7 MONOFARG autoradiographs of ^{125}I-FITC-Con-A-labeled, freeze-dried and shadowed RBCG's (*A, B*) and paired freeze-fractured and shadowed RBC's (*C, D*). (*A*) Portions of two RBCG's. (*B*) RBCG showing large area of single membrane, cytoplasmic surface, *PS*, surrounded by an area two membranes thick with exposed extracellular surface, *ES*. (*C, D*) Identical micrographs of portions of five split erythrocyte membranes (*EF*) identified and outlined in (*D*) to illustrate how silver grain densities were determined by grain counting and planimetry. All samples were exposed for 63 d, developed in D-19, 4 min, 20°C. × 8,900.

(adjusted for dose, background subtracted) is linearly proportional to the number of molecules (number of decays) per unit area.

Transmembrane Distribution

Autoradiographs of collapsed and flattened lysed RBC's labeled with ^{125}I-FITC-Con-A are shown in Fig. 7*A* and *B*. Ghosts that appeared minimally ruptured (Fig. 7*A*) were usually smaller than others, apparently swollen before lysis, that displayed large areas of cytoplasmic surface (PS) (Fig. 7*B*). Grain densities over single membranes, PS regions, and over double membranes, ES regions, were tabulated. Inspection of numerous micrographs such as those in Fig. 7 indicated that MONOFARG resolution was high enough to allow tabulation of grain densities over PS areas as shown in Fig. 7*B* without correction for radiation spread. This assumption becomes increasingly valid as the PS area increases. Fig. 7*C* and *D* are duplicate prints of the same autoradiograph of a split RBC preparation, except that E-faces are outlined and identified in Fig. 7*D*. Both the RBCG's (Fig. 7*A*, *B*) and split RBC's (Fig. 7*C*, *D*) were prepared from the same ^{125}I-FITC-Con-A-labeled cell preparation and processed identically for shadowing, exposure, photography, and microscopy. Although there was no gross indication of in-plane heterogeneity of silver grain distribution (*i.e.*, numbers of grains were proportional to area), there was a distinct variation in grain density from cell to cell.

Grain density data for unsplit ghosts in regions one or two membranes thick and for split membrane E-faces are given in Fig. 8. The grain densities over regions of double membrane

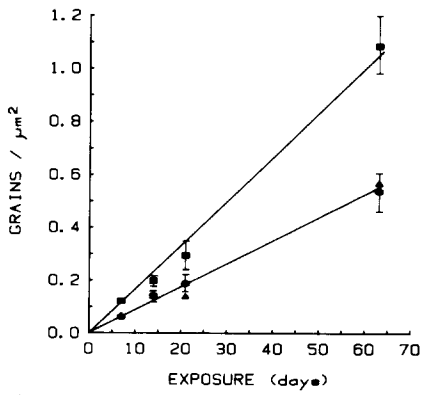

FIGURE 8 Silver grain density over unsplit and split erythrocyte membranes as a function of dose (exposure time). Data from unsplit membranes of double thickness (■) or single thickness (▲) and from split membrane E-faces (●) are plotted. Means ± SE given for double and split membranes.

were corrected for loss of radioactivity during ghosting. Measurements of cpm by LSC, and numbers of RBC's and RBCG's by quantitative light microscopy, indicated that ~15% of the ^{125}I-FITC-Con-A was removed during ghosting of RBC's attached to PL-glass. Corrected grain densities for the double membranes at each of the four exposure times (7, 14, 21, and 63 d) are close to twice those of the single membranes. For example, at 63 d the uncorrected grain density for double membranes is 0.934 (1,295 grains/1,387 μm^2 measured), 1.083 after correction for lysis and background; for single membrane, 0.584 (328 grains/562 μm^2 measured), 0.568 after correction; and for split membrane E-faces, 0.540 (1,702 grains/3,150 μm^2 measured), 0.525 after correction. The grain densities of single membranes and of split membrane E-faces are essentially identical, indicating that all of the ^{125}I-FITC-Con-A resides on the extracellular surface of the membrane and remains there during freeze-fracturing. The large standard error bars (Fig. 8) reflect the wide range of grain densities among the populations of RBCG's and split RBC's.

DISCUSSION

Three aspects of MONOFARG have been presented in this report. Details of the method have been described for the first time. ^{125}I test systems have been used to evaluate the efficiency and quantitative features of the method. And the method has been used to determine the sidedness after freeze-fracturing of ^{125}I-FITC-Con-A applied to RBC membranes.

The autoradiographic component of MONOFARG is based on a modified stripping film technique (13, 24, 27, 49) following the principles of the flat substrate method (5, 6, 31, 37–39) of emulsion monolayer preparation. It differs from most other methods in that the Parlodion supporting film lies between the source and the detector. Advantages to such a location are that the Parlodion can act as an additional barrier to chemographic artifacts (13, 35) and that the emulsion is in direct contact with photographic chemicals. A disadvantage is that, by increasing the distance between source and detector, both sensitivity and resolution could be adversely affected (7, 8, 27, 39, 44). However, the ^{125}I efficiency data collected in the present study, and a comparison of conventional TEM ARG geometry with that of MONOFARG, suggest that this may not be a serious problem. Although it is clear that a 100-nm thick test specimen is not always optimum, it has been noted (12, 36) that minimum error is introduced if ^{125}I test specimens for TEM ARG sensitivity evaluation are "at the upper end of the thickness scale used (*i.e.*, 1,000 Å)" (reference 12, p. 86). The thickness of split membrane (~5 nm) plus Pt-C replica (5 nm) plus carbon (5–20 nm) plus gelatin-subbed Parlodion (50–100 nm) is comparable (total maximum thickness = 130 nm). However, Junger and Bachmann (27) have noted that a 20-nm thick layer of collodion between ^{125}I and Ilford L4 emulsion decreased the efficiency by ~10% with Microdol-X development. Although the effect of the Parlodion film on resolution appears qualitatively minor, the resolution of MONOFARG has yet to be unambiguously determined. For qualitative and high-resolution detection of nondiffusible radioisotopes such as concanavalin A, liquid emulsion could be applied directly to the replica. However, for quantitative studies such direct coating would probably not be suitable due to variability in emulsion thickness and hydration-induced relocation of extractable or diffusible isotopes.

Each of the two systems used to evaluate quantitative aspects of ^{125}I MONOFARG had its own set of assumptions and sources of error. In the ^{125}I-FITC-Con-A-treated PL-glass test system the greatest potential error was in determining the surface concentration of the isotope in dpd/μm^2. The assumption that the surface concentration was homogeneous was not totally valid, since measurements of the peripheral 0.5 mm edges of 11 × 22-mm glasses showed more variable and usually higher levels of radioactivity per unit area of glass. In addition, accurate measurement of surface activity was hampered by poor recovery of the Con A aggregates from the dried PL-glass surface. In the ^{125}I-labeled RBC system, recovery was less of a problem. Spectroscopic and isotopic data (22) have shown that >95% of the activity could be recovered from the freeze-dried samples. However, by electron microscope standards, the

amount of Con A bound can vary significantly from cell to cell, thus generating large error bars in grain density evaluations. The RBC experiments were similar to most other efficiency evaluations in that the specific activity, here dpd/μm^2 ES, was determined before preparation of the monolayer for ARG processing. This is comparable to measuring specific activity of radiolabeled plastics (1, 41, 43) before embedding and sectioning, or of bovine serum albumin solutions before preparing dry films (12). Furthermore, it was assumed that specific activity of the ^{125}I-FITC-Con-A was the same before and after monolayer formation, fracturing, and shadowing, that the in-plane distribution was random, and that the isotope partitioned exclusively with the E-face. These assumptions were tested and found to be true.

The efficiency of ^{125}I MONOFARG was surprisingly high. For example, for doses less than one disintegration/μm^2, mean efficiency was 25% for the PL-glass experiments and 44% for the RBC experiments. However, why are these efficiencies so different? In both cases the same isotope, ^{125}I-FITC-Con-A, was examined. Part of the difference must be due to the assumptions and potential errors mentioned above. The PL-glass efficiencies were probably low. Edges of the glass were more radioactive than centers. This would have produced more cpm's by LSC than would have been detected by MONOFARG sampling. In addition, the PL-glass and RBC experiments were totally independent. Thus, variation in replica thickness, emulsion thickness, and photographic processing may be responsible for the wide range of efficiencies. Future experiments will examine such variables.

The high efficiency was especially surprising for two reasons. First, to ensure good resolution, the MONOFARG emulsion monolayers were made thinner than the thickness known to produce highest efficiency (12). And second, the electron-scattering Pt-C replica was expected to decrease detection efficiency significantly, because even heavy metal staining reduces ^{125}I efficiency by ~15% (12, 44). However, that was not the case in the present study. Comparison of unshadowed with paired shadowed PL-glass surfaces (Fig. 4*A*, *B*) showed only a 17% decrease in efficiency from 24% to ~20% (Fig. 5*B*, *C*).

The dose response of MONOFARG to ^{125}I using D-19 development was qualitatively similar to that previously reported for nonshadowed samples using gold latensification followed by Elon-ascorbic acid development (12). For the PL-glass test system there was a clear decrease in MONOFARG efficiency with increasing dose (Fig. 5*B*, *C*). Decreasing efficiency may in part explain the low efficiency values of 3.4% to 5.6% reported by Nermut and Williams (30) for a modified version of MONOFARG examining much higher doses.

In the transmembrane analysis presented here, MONOFARG was used to determine the distribution of ^{125}I-FITC-Con-A in two ways: first, by comparing the grain density of the intact single membrane to that of the split membrane; and second, by comparing the number of grains per cell to the calculated number of grains per total area of extracellular surface. Although both determinations gave similar results, the first approach will probably be more generally applicable. Many cells and organelles can be attached to polylysine-treated surfaces (9, 10, 26, 28, 29), and such preparations are suitable for MONOFARG. More importantly, a direct comparison of intact single membrane with its split counterpart circumvents the necessities of measuring the amount of isotope before and after lysis, and of knowing or determining the total E-surface area of the plasma membrane. Use of MONOFARG for transmembrane analysis relies on the assumption that the radioactivity is randomly distributed in the plane of the autoradiographed membrane. In the present study, ^{125}I-FITC-Con-A was found to be so distributed. The number of silver grains was directly proportional to the area of unsplit or split membrane.

In the present study, because both intact and split membranes produced identical grain densities, corrections for dose or isotope concentration dependence were not required. However, it was not known whether grain density would be proportional to isotope concentration in the presence of a Pt-C replica, or not, and, if so, over what dose range. Such information was included in the present report and may be essential to future MONOFARG studies of the transmembrane distribution of ^{125}I where grain densities of unsplit and split membrane differ significantly; i.e., where most of the isotope partitions with the cytoplasmic side during fracturing.

Although the resolution of MONOFARG for ^{125}I has yet to be carefully evaluated, a preliminary indication could be derived from the membrane preparations (20). Widely spaced RBCG's, flattened against PL-glass, were treated as disk sources of radioactivity of uniform distribution. The shortest distance between silver grains overlying PL-glass and the edge of the membrane was measured (up to 1.2 μm^2). Grains were accumulated in bins of 30 nm and integrated grain counts plotted versus distance. From this analysis the preliminary HD value was ~150 nm. A similar value was obtained using the "successive hypothesis testing" approach of Salpeter et al. (43) where expected grain densities were compared with densities observed. When an HD value of 150 nm was used, the observed data approximately fit the expected distribution from a solid disk of infinite diameter uniformly labeled with ^{125}I. It should be emphasized, however, that the 150-nm value is quite tentative. It is likely that, as definitive resolution data accumulate, the real value will approach the ~90-nm value for ^{125}I determined by Salpeter et al. (44).

In summary, details of the technique of MONOFARG, a quantitative evaluation of its efficiency, and an evaluation of the sidedness of ^{125}I-FITC-Con-A have been described. Other isotopes that are routinely used for TEM ARG, such as ^{3}H and ^{14}C, remain to be similarly evaluated. Monolayer freeze-fracturing, a tool for membrane fractionation, has been used in the present study for cytochemical evaluation of the transmembrane distribution of an ^{125}I probe. Although MONOFARG is limited to an examination of plasma membranes or isolated membrane fractions and thus differs from other recent cytochemical methods using freeze-fracture (11, 32, 33), it has unique potential. MONOFARG should provide quantitative information about both the transmembrane and in-plane distributions of a wide variety of radioisotopically labeled molecules.

I thank Mrs. Eleanor Crump for excellent technical assistance and Dr. Walther Stoeckenius for continued support (NIH GM27057).

This work was supported by grant GM27049 from the National Institutes of Health (NIH), and was done during the tenure of an Established Investigatorship of the American Heart Association and with funds contributed in part by the San Francisco Chapter of the American Heart Association, California Affiliate.

Received for publication 29 July 1981, and in revised form 7 December 1981.

Note Added in Proof: A mini-review of FARG and MONOFARG literature and approaches, written after this report, is currently in press:

Fisher, K. A. 1982. Monolayer freeze-fracture autoradiography: origins and directions. *J. Microsc. (Oxf).*

REFERENCES

1. Bachmann, L., M. M. Salpeter, and E. E. Salpeter. 1968. Das Auflösungsvermögen electronenmikroskôpischer Autoradiographien. *Histochemie.* 15:234–250.
2. Bogoroch, R. 1972. Liquid emulsion autoradiography. *In:* Autoradiography for Biologists. P. B. Gahan, editor. Academic Press, Inc., NY. 65–94.
3. Bolton, A. E., and W. M. Hunter. 1973. The labeling of proteins to high specific radioactivities by conjugation to a ^{125}I-containing acylating agent. *Biochem. J.* 133:529–539.
4. Branton, D., S. Bullivant, N. B. Gilula, M. J. Karnovsky, H. Moor, K. Mühlethaler, D. H. Northcote, L. Packer, B. Satir, P. Satir, V. Speth, L. A. Staehelin, R. L. Steere, and R. S. Weinstein. 1975. Freeze-etching nomenclature. *Science (Wash. D. C.).* 190:54–56.
5. Budd, G. C. 1972. High resolution autoradiography. *In:* Autoradiography for Biologists. P. B. Gahan, editor. Academic Press, Inc., NY. 95–118.
6. Budd, G. C., and S. R. Pelc. 1964. The membrane method of electron microscope autoradiography. *Stain Technol.* 39:295–302.
7. Caro, L. G. 1962. High resolution autoradiography. II. The problem of resolution. *J. Cell Biol.* 15:189–200.
8. Caro, L. G., R. P. Van Tubergen, and J. A. Kolb. 1962. High-resolution autoradiography. I. Methods. *J. Cell Biol.* 15:173–188.
9. Clarke, M., G. Schatten, D. Mazia, and J. A. Spudich. 1975. Visualization of actin fibers associated with the cell membrane in amoebae of *Dictyostelium discoideum. Proc. Natl. Acad. Sci. U. S. A.* 72:1758–1762.
10. Cohen, C. M., D. I. Kalish, B. S. Jacobson, and D. Branton. 1977. Membrane isolation on polylysine-coated beads. *J. Cell Biol.* 75:119–134.
11. Elias, P. M., D. S. Friend, and J. Goerke. 1979. Membrane sterol heterogeneity. Freeze-fracture detection with saponins and filipin. *J. Histochem. Cytochem.* 27:1247–1260.
12. Fertuck, H. C., and M. M. Salpeter. 1974. Sensitivity in electron microscope autoradiography for ^{125}I. *J. Histochem. Cytochem.* 22:80–87.
13. Fisher, K. A. 1974. Freeze-fracture autoradiography: a method to study biomembranes. Ph.D. Dissertation. University of California, Berkeley, CA. 220p.
14. Fisher, K. A. 1975. "Half" membrane enrichment: verification by electron microscopy. *Science (Wash. D. C.).* 190:983–985.
15. Fisher, K. A. 1976. Analysis of membrane halves: cholesterol. *Proc. Natl. Acad. Sci. U. S. A.* 73:173–177.
16. Fisher, K. A. 1976. Autoradiography of membrane "halves": ^{3}H-cholesterol labeled erythrocytes. *J. Cell Biol.* 70(2, Pt. 2):218*a* (Abstr.).
17. Fisher, K. A. 1978. Split membrane lipids and polypeptides. *In:* Electron Microscopy 1978. Vol. III. J. M. Sturgess, editor. Proc. Ninth Internatl. Cong. E.M., Toronto. 521–532.
18. Fisher, K. A. 1980. Split membrane analysis. *Annu. Rev. Physiol.* 42:261–273.
19. Fisher, K. A. 1980. "Half" membranes: rapid quantitative concentration assays. *Fed. Proc.* 39:1985 (Abstr.).
20. Fisher, K. A. 1981. Monolayer freeze-fracture autoradiography: preliminary estimates of 125-I resolution. *J. Cell Biol.* 91(2, Pt. 2):249*a* (Abstr.).
21. Fisher, K. A. 1982. Preparation of planar membrane monolayers for spectroscopy and electron microscopy. *Methods Enzymol.* In press.
22. Fisher, K. A. 1982. Spectroscopic assays for measuring quantities of erythrocyte membrane "halves." *J. Cell Biol.* 92:44–52.
23. Fisher, K., and D. Branton. 1973. Freeze-fracture autoradiography: a method for studying biomembranes. *J. Cell Biol.* 59(2, Pt. 2):99*a* (Abstr.).
24. Fisher, K. A., and D. Branton. 1976. Freeze-fracture autoradiography: feasibility. *J. Cell Biol.* 70:453–458.
25. Forberg, S., E. Odeblad, R. Söremark, and S. Ullberg. 1964. Autoradiography with isotopes emitting internal conversion electrons and auger electrons. *Acta Radiologica.* 2: 241–262.
26. Jacobson, B. S., and D. Branton. 1977. Plasma membrane: rapid isolation and exposure of the cytoplasmic surface by use of positively charged beads. *Science (Wash. D. C.).* 195: 302–304.
27. Junger, E., and L. Bachmann. 1980. Methodological basis for and autoradiographic demonstration of insulin receptor sites on the surface of whole cells: a study using light- and scanning electron microscopy. *J. Microsc. (Oxf).* 119:199–211.
28. Kalish, D. I., C. M. Cohen, B. S. Jacobson, and D. Branton. 1978. Membrane isolation on polylysine-coated glass beads: asymmetry of bound membrane. *Biochim. Biophys. Acta.* 506:97–110.
29. Mazia, D., G. Schatten, and W. Sale. 1975. Adhesion of cells to surfaces coated with polylysine. Applications to electron microscopy. *J. Cell Biol.* 66:198–200.
30. Nermut, M. V., and L. D. Williams. 1980. Freeze fracture autoradiography of the red blood cell plasma membrane. *J. Microsc. (Oxf).* 118:453–461.
31. Pelc, S. R., J. D. Coombes, and G. C. Budd. 1961. On the adaptation of autoradiographic techniques for use with the electron microscope. *Exp. Cell Res.* 24:192–195.
32. Pinto da Silva, P., C. Parkison, and N. Dwyer. 1981. Fracture-label: cytochemistry of freeze-fracture faces in the erythrocyte membrane. *Proc. Natl. Acad. Sci. U. S. A.* 78:343–347.
33. Rash, J. E. 1979. The sectioned replica technique: direct correlation of freeze-fracture replicas and conventional thin-section images. *In:* Freeze-fracture: Methods, Artifacts, and Interpretations. J. E. Rash and C. S. Hudson, editors. Raven Press, NY. 153–160.
34. Rix, E., A. Schiller, and R. Taugner. 1976. Freeze-Fracture-Autoradiography. *Histochemistry.* 50:91–101.
35. Rogers, A. W. 1969. Techniques of Autoradiography. 2nd edition. Elsevier Publishing Co., NY. 338p.
36. Salpeter, M. M. 1973. Sensitivity in electron microscope autoradiography. II. Effect of heavy metal staining. *J. Histochem. Cytochem.* 21:623–627.
37. Salpeter, M. M., and L. Bachmann. 1964. Autoradiography with the electron microscope. *J. Cell Biol.* 22:469–477.
38. Salpeter, M. M., and L. Bachmann. 1965. Assessment of technical steps in electron microscope autoradiography. *In:* The Use of Radioautography in Investigating Protein Synthesis. C. P. Leblond and K. B. Warren, editors. Academic Press, Inc., NY. 32–41.
39. Salpeter, M. M., and L. Bachmann. 1972. Autoradiography. *In:* Principles and Techniques of Electron Microscopy. Vol. 2. M. A. Hayat, editor. Van Nostrand and Reinhold Co., NY. 219–278.
40. Salpeter, M. M., and F. A. McHenry. 1973. Electron microscope autoradiography. *In:* Advanced Techniques in Biological Electron Microscopy. J. K. Koehler, editor. Springer-Verlag, NY. 113–152.
41. Salpeter, M. M., and E. E. Salpeter. 1971. Resolution in electron microscope radioautography. II. Carbon^{14}. *J. Cell Biol.* 50:324–332.
42. Salpeter, M., and M. Szabo. 1972. Sensitivity in electron microscope radioautography using Ilford L4 emulsion: the effect of radiation dose. *J. Histochem. Cytochem.* 20:425–434.
43. Salpeter, M. M., L. Bachmann, and E. E. Salpeter. 1969. Resolution in electron microscope radioautography. *J. Cell Biol.* 41:1–20.
44. Salpeter, M. M., H. C. Fertuck, and E. E. Salpeter. 1977. Resolution in electron microscope autoradiography. III. Iodine-125, the effect of heavy metal staining, and a reassessment of critical parameters. *J. Cell Biol.* 72:161–173.
45. Salpeter, M. M., F. A. McHenry, and E. E. Salpeter. 1978. Resolution in electron microscope autoradiography. IV. Application to analysis of autoradiographs. *J. Cell Biol.* 76:127–145.
46. Schiller, A., E. Rix, and R. Taugner. 1978. Freeze fracture autoradiography. *Mikroskopie.* 34:24–28.
47. Schiller, A., E. Rix, and R. Taugner. 1978. Freeze-fracture autoradiography: the *in vacuo* coating technique. *Histochemistry.* 59:9–16.
48. Schiller, A., R. Taugner, and E. Rix. 1979. Freeze-fracture autoradiography. Progress towards a routine technique. *J. Histochem. Cytochem.* 27:1514–1515.
49. Williamson, J. R., and H. Van den Bosch. 1971. High resolution autoradiography with stripping film. *J. Histochem. Cytochem.* 19:304–309.